Vol. 20, No. 1 (2021) 51-66
Revista Mexicana de Ingeniería Química

Concentration estimation and fault tolerant control in a CSTR modelled as a quasi linear parameter varying system

Estimación de concentración y control tolerante a fallas en un CSTR modelado como un sistema quasi lineal con parámetros variables

G. Ortiz-Torres, J.Y. Rumbo-Morales, F.D.J. Sorcia-Vázquez, A.F. Pérez-Vidal*, A. Cruz-Rojas, J.A. Brizuela-Mendoza, E. Oceguera-Contreras

Universidad de Guadalajara. Centro Universitario de los Valles. Carretera Guadalajara-Ameca Km. 45.5 C.P. 46600, Ameca, Jalisco, México.

Received: February 20 2020; Accepted: May 15, 2020

Abstract

A design of a product concentration estimation and a Fault Tolerant Control (FTC) strategy for compensate an actuator fault in a Continuous Stirred Tank Reactor (CSTR) are developed in this paper. Second and third-order CSTR systems are considered to validate the proposed FTC scheme. Furthermore, a comparison between nonlinear, linear and quasi Linear Parameter Varying (qLPV) models for both CSTR systems are presented. The results demonstrate that the qLPV representation reproduce the nonlinear, in the selected segment, better than the linear model. Then, a Proportional-Integral Observer (PIO) is designed using the qLPV representation in order to estimate the states and the actuator fault presented in the process. These estimations are used by the FTC system for compute a new control law using a Linear Matrix Inequality (LMI) to ensure the stability of both the qLPV PIO and the FTC law. Thus, the main contributions of this work are four: i) to propose a new representation of the second and three-order CSTR nonlinear model by means of a qLPV system, preserving the nonlinear dynamics of the original nonlinear model, ii) to exploit the easiness to extend theoretical results that originally were conceived for linear systems, to qLPV systems, iii) to estimate the product concentration in order to generate a new FTC law, and iv) to validate in simulation the FTC scheme to reduce the effect of an actuator fault in a CSTR process.

Keywords: Fault tolerant control, fault estimation, quasi linear parameter varying, continuous stirred tank reactor.

Resumen

En el presente artículo se desarrolla el diseño de un estimador de concentración y una estrategia de Control Tolerante a Fallas (FTC) para compensar la falla en un actuador de un Reactor tipo Tanque Continuamente Agitado (CSTR). Para validar el esquema de FTC se considera un sistema de CSTR de segundo y de tercer orden. Además, se presenta una comparación entre los modelos no lineal, lineal y quasi Lineal con Parámetros Variables (qLPV) de ambos sistemas CSTR. Los resultados demuestran que la representación qLPV reproduce mejor el comportamiento no lineal de los sitemas CSTR, en el segmento seleccionado, en comparación con el modelo lineal. Posteriormente, se diseña un Observador Proporcional-Integral (PIO) utilizando la representación qLPV para estimar los estados y la falla en el actuador del proceso. Estas estimaciones son computadas para generar una nueva ley de control utilizando una Desgualdad Matricial Lineal (LMI) para asgurar la estabilidad del PIO qLPV y de la ley de FTC. Así, las principales contribuciones de este trabajo son cuatro: i) proponer una nueva representación para el sistema no lineal del CSTR de segundo y tercer orden utilizando un sistema qLPV, el cual preserva las dinámicas no lineales del modelo no lineal original. ii) aprovechar la facilidad de extender los resultados teóricos, originalmente concebidos para los sistemas lineales, iii) estimar la concentración del CSTR para generar una nueva ley de control tolerante a fallas, y iv) validar el esquema FTC en simulación para reducir el efecto de la falla en un CSTR.

Palabras clave: Control tolerante a fallas, estimación de fallas, quasi lineal con parámetros variables, reactor tipo tanque continuamente agitado.

* *Corresponding author. E-mail*: alanperezvidal@hotmail.com
https://doi.org/10.24275/rmiq/Sim1379
ISSN:1665-2738, *issn-e*: 2395-8472

Nowadays, chemical industry is characterized by large plants with complex arrangement of processing units and highly integrated with respect to material and energy flows (Daher *et al.,* 2020; Rumbo-Morales *et al.,* 2018, 2020). Given these characteristics and with the increase of requirement performances at different operation conditions, the modern industrial systems have become progressively vulnerable to faults which inevitably influence the dynamics of the process stability, reliability, and safety (Sorcia-Vázquez *et al.,* 2020). Also, external disturbances can lead to different faults, such as actuator stuck, actuator degradation, voltage control failure, structural damage, physical aging, and fatigue, which can change the states of the process (Llanes-Santiago *et al.,* 2019).

In order to identify malfunctions at any time and to improve reliability and safety in a process, Fault Tolerant Control (FTC) methods can be considered. The FTC techniques are classified into two types (Amin *et al.,* 2019): passive and active. On one hand, in the passive techniques, a fixed controller is designed for tolerating changes of the plant dynamics and then, the stabilized system could satisfy its goals under all faulty conditions. This approach needs neither Fault Diagnosis (FD) schemes nor controller reconfiguration, but it has limited capabilities because it uses fixed parameters. On the other hand, in the active techniques the controller parameters are adapted or reconfigured according to the fault using the information of the FD system, so that the stability and acceptable performance of the system can be maintained. According to Blanke *et al.,* (2006), different names can be used to distinguish the diagnostic steps: fault detection, fault isolation and fault identification (also known as fault estimation).

In the context of fault detection and isolation applied to a chemical systems, Wang *et al.,* (2020) presents a novel deep learning based fault diagnosis scheme in chemical processes. The effectiveness and performance of the proposed method have been demonstrated in simulation. In Gholizadeh *et al.,* (2019) a fault detection and identification algorithm is proposed for a Continuous Stirred Tank Reactor (CSTR) by combining the extended Kalman filter and neuro-fuzzy networks. Simulation results show that the proposed methodology is very effective to detect and identify the faults of the system in different faulty modes. A model based robust observer for fault estimation in a CSTR was investigated in Boudjella and Illoul, (2019). They propose a combination of two super-twisting observers for state estimation and fault reconstruction using a linear model of the CSTR. The effectiveness and robustness of the scheme are illustrated in simulation. In Zerari and Chemachema, (2019) a robust controller is implemented using a neural network designed for a uncertain CSTR system with input nonlinearities and external disturbance. This external disturbance can be considered as an external fault. In this context, a sensor fault detection system for a CSTR process is presented in Zhang *et al.,* (2020). They consider the CSTR plant as a stochastic linear time-varying system with parameter uncertainty and limited resolution. Simulation results are carried out to illustrate the validity of the proposed method. In Adam-Medina *et al.,* (2013) a fault detection scheme using second-order sliding model observers applied to a double pipe heat exchanger is proposed. Similar work is presented in García-Morales *et al.,* (2015), by designing a FD system based on a super-twisting sliding mode observers for a double pipe heat exchanger. Experimental results have shown the effectiveness of the estimation and isolation of a fault in one inlet and two outlet sensors of the heat exchanger.

Usually the mathematical model of a CSTR is represented by a set of ordinary differential equations (Zheng *et al.,* 2020; Alshammari *et al.,* 2020; Boudjella and Illoul, 2019) or linear approximations (Hernández-Osorio *et al.,* 2020; Yazdi and Khayatian, 2020; Simkoff and Baldea, 2019). However an alternative to represent its nonlinear dynamic is through a collection of linear subsystems. Recently, Linear Parameter Varying (LPV) systems have garnered much interest (Marx *et al.,* 2019). The importance of this representation is that the LPV mathematical model is able to exactly represent or approximate the nonlinearities by a set of linear models blended by scheduling functions. It is important to remark that the polytopic LPV and Takagi-Sugeno (T-S) systems are described by the same form (Rotondo *et al.,* 2015). In fact, in Tanaka *et al.* (2006) it is established that the T-S model is a special case of an LPV model. Nevertheless, the community of researchers working on T-S models uses the name "T-S fuzzy systems", even if the obtained model is no "fuzzy" because the weighting functions are completely deterministic that corresponds to LPV systems as detailed in Rodrigues *et al.* (2014). In the literature there are two known methods to obtain LPV models, the linearization and the sector-nonlinear approach. Some application of the LPV control theory to a CSTR using linearization approach have been presented in Tamboli and Chile (2018). However, the main drawback is that there is no general method to

select the linearization points (Ahammed and Azeem, 2019).

A more accurate representation of the nonlinear system can be obtained by considering the sector-nonlinearity approach, also known as quasi-LPV (qLPV) because the scheduling functions are represented by nonlinear state or input dependent functions. The main advantage of this approach is that the qLPV model is an exact representation of the nonlinear system in the selected sector (Martínez-Garctía *et al.,* 2020; Ohtake *et al.,* 2003). For instance, in Alshammari *et al.* (2019), an advanced fuzzy logic Proportional-Integral-Derivative (PID) based control technique has been designed for a fuzzy representation of a CSTR; simulation results show a more accurate tracking for the desired output trajectory than a classical PID controller. In Ebrahimi *et al.* (2019) a parallel distributed compensation-based for a CSTR modelled as a qLPV have been presented. Simulation results corroborate that the designed controllers, in term of Linear Matrix Inequalities (LMI), ensure the global stability of the closed-loop system. A Sensor fault tolerant control strategy for a CSTR under modelling uncertainties is presented in Abdullah and Zribi (2013). The authors have designed a qLPV observer to estimate both the unmeasured system states and the sensor fault. Simulation results illustrate the developed theoretical results. Recently, a fault detection for uncertain CSTR plant, modelled as a LPV system, is developed in Wan *et al.* (2020). A probabilistic set-membership parity relation approach is proposed to exploit probabilistic information on the parametric uncertainties; the effectiveness of the proposed approach is illustrated in simulation. To deal with fault reconstruction, Asadi *et al.* (2020), present a robust sliding mode observer for a CSTR modelled as a T-S system. Simulation results demonstrated the effectiveness of the proposed strategy in reconstructing actuator faults.

In order to highlight the novelty of this paper, a comparison of fault tolerant strategies applied to a CSTR system is presented in Table 1. It is clear that even the works reported in the literature, there are few works based on qLPV representation for the design of active fault tolerant controllers to the CSTR system, therefore this problem remains important and a challenge to be solved in a theoretical and practical way.

The main contributions of this work are four: i) to propose a new representation of the second and three-order CSTR nonlinear model by means of a qLPV system, preserving the nonlinear dynamics of the original nonlinear model. This new representation allows to increase the range of applications of control algorithms for CSTR systems, ii) to exploit the easiness to extend theoretical results that originally were conceived for linear systems, to qLPV systems, iii) to estimate the product concentration in order to generate a new FTC law, and finally iv) to validate in simulation the active FTC scheme to reduce the effect of an actuator fault in a CSTR process.

1 Materials and methods

1.1 Preliminaries of qLPV systems

The qLPV representation of the CSTR is obtained using the sector-nonlinearity technique, proposed in Ohtake *et al.* (2003). In this section, preliminaries of the qLPV modelling are presented. Then, the sector-nonlinearity technique is applied to the CSTR system in order to design the FTC system.

Table 1. Quality comparison of fault tolerant strategies applied to a CSTR system.

Characteristic	References							
	[1]	[2]	[3]	[4]	[5]	[6]	[7]	Our work
Avoid complicated implementation	×	✓	✓	✓	×	×	✓	✓
State estimation algorithm	✓	✓	×	✓	✓	×	×	✓
Fault detection, isolation or estimation	✓	✓	✓	✓	✓	✓	✓	✓
An active fault tolerant controller design	×	×	×	×	×	×	×	✓

[1] Gholizadeh *et al.* (2019); [2] Boudjella and Illoul (2019); [3] Abdullah and Zribi (2013); [4] Wan *et al.* (2020); [5] Zerari and Chemachema (2019); [6] Zhang *et al.* (2020); [7] Asadi *et al.* (2020).

Consider a nonlinear system described by

$$\begin{aligned} \dot{x} &= f(x)x + g(x)u + a, \\ y &= h(x)x, \end{aligned} \tag{1}$$

where f, g and h are smooth nonlinear functions with respect to the states, a represents a constant vector, x is the state vector, u is the input vector of the system and y denotes the measurable output vector. By considering the sector-nonlinearity technique, the nonlinear system Eq. (1) is exactly represented only in a convex set, by the qLPV model given by:

$$\begin{aligned} \dot{x} &= \sum_{i=1}^{m} \rho_i(\zeta)(A_i x + B_i u) + a, \\ y &= \sum_{i=1}^{m} \rho_i(\zeta)(C_i x), \end{aligned} \tag{2}$$

where A_i, B_i and C_i are constant matrices of the proper dimensions associated to each local model of the system i, with $i = 1, 2, \ldots, m$. The scheduling functions ρ_i are nonlinear and depend on the decision variable ζ which is represented by the non-constant terms in f, g and h in Eq. (1). The number of local linear models is directly related to the number of the nonlinear terms. For each nonlinear term, two sub-models are obtained such that for p nonlinear terms, the global model is composed of $m = 2^p$ sub-models. The construction of the scheduling functions satisfy the following convex set sum property:

$$\begin{aligned} &0 \leq \rho_i(\zeta) \leq 1, \ \forall t, \forall i = 1, 2, \ldots, m, \\ &\sum_{i=1}^{m} \rho_i(\zeta) = 1, \ \forall t. \end{aligned} \tag{3}$$

Note that Eq. (1) is not unique and therefore the qLPV representation of the nonlinear system expressed in Eq. (2) obtained by the sector-nonlinearity approach is not unique. For each scheduling variable $\zeta_j(t) \in [\underline{\zeta}_j, \overline{\zeta}_j]$ with $j = 1, 2, \ldots, p$, there are two weighting functions μ_0^j, μ_1^j which are expressed as:

$$\mu_0^j(\zeta_j) = \frac{\overline{\zeta}_j - \zeta_j(t)}{\overline{\zeta}_j - \underline{\zeta}_j}, \quad \mu_1^j(\zeta_j) = 1 - \mu_0^j, \tag{4}$$

where $\underline{\zeta}_j$ and $\overline{\zeta}_j$ are the minimum and maximum values of the non-constant terms, respectively. In this paper, it is considered that the scheduling variable $\zeta_j(t)$ is measurable. Then, the scheduling functions for each local mathematical model are defined as:

$$\rho_i(\zeta_j) = \prod_{j=1}^{p} \mu_\gamma^j(\zeta_j), \ i = 1, 2, \ldots, m, \tag{5}$$

where the index γ is zero or one, depending on which local scheduling function is considered and indicate which portion of the j-th scheduling variable is involved in the i-th sub-model. Consequently, by using the scheduling functions given by Eq. (5), the nonlinear system Eq. (1) is exactly represented in the selected segment Eq. (3) by the qLPV model expressed in Eq. (2).

1.2 Nonlinear model of the CSTR

The CSTR plant configuration is presented in Fig. *1.2*. The dynamic modeling equations to find the tank and jacket temperature are established using the following assumptions (Seborg *et al.,* 2010):

- The thermal capacitances of the coolant and the cooling coil wall are negligible compared to the thermal capacitance of the liquid in the tank,
- The volume and liquids are constant with constant density. Perfect mixing is assumed in both tank and jacket. The heat of mixing is negligible compared to the heat of reaction,
- The rate of heat transfer from the jacket to the tank is governed by the equation $-UA(T - T_j)$, where U is the overall heat transfer coefficient and A is the area for heat transfer.

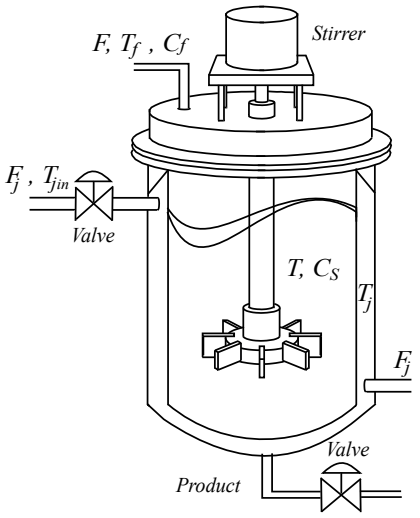

Fig. 1. CSTR configuration.

Table 2. CSTR symbols and values (Seborg *et al.,* 2010).

Description	Symbol	Value	Unit	Description	Symbol	Value	Unit
Inlet temperature	T_{jin}	283	K	Heat Capacity (HC)	c_p	0.239	J/g K
CSTR volume	V	100	L	Cooler water HC	c_{pj}	0.239	J/g K
Cooler volume	V_j	50	L	Process flow rate	F	100	L/min
Activation energy term	E/R	8750	K	Feed concentration	C_f	1	mol/L
Reaction rate constant	k_0	7.2×10^{10}	min^{-1}	Cooler flow rate	F_j		L/min
Heat transfer term	UA	5×10^4	J/min K	Product concentration	C_S		mol/L
Heat of reaction	$-\Delta H$	5×10^4	J/mol	Cooler temperature	T_j		K
Liquid density	ϱ	1000	g/L	CSTR temperature	T		K
Cooler water density	ϱ_j	1000	g/L	Temperature of feed	T_f		K

[1] The simulated value of these parameters are different for the second and the third-order CSTR system.

The nonlinear model of the CSTR is based on the mass and energy balance and it is expressed as a differential equation with a nonlinear third-order dynamic model, as follows:

$$\dot{T} = \frac{F}{V}(T_f - T) - \frac{UA}{V\varrho c_p}(T - T_j) - \frac{\Delta H}{\varrho c_p} r C_S, \quad (6a)$$

$$\dot{T}_j = \frac{F_j}{V_j}(T_{jin} - T_j) + \frac{UA}{V_j \varrho_j c_{pj}}(T - T_j), \quad (6b)$$

$$\dot{C}_S = \frac{F}{V}(C_f - C_S) - r C_S, \quad (6c)$$

where

$$r = k_0 e^{(-E/RT)} \quad (7)$$

is the specific reaction rate, T is the reaction temperature of the CSTR product, T_j is the coolant temperature entering into the thermal jacket, T_f is the temperature of the substrate entering the reactor and T_{jin} is the temperature of cooler inlet. The heat of the reaction is represented by ΔH, k_0 denotes the reaction rate constant, E is the activation energy and R represents the molar gas constant. The concentration of the product inside the CSTR is C_S, C_f denotes the feed concentration, F represents the volumetric flowrate, V is the CSTR volume, ϱ and ϱ_j are the density of the mass of reaction and the density of cooling agent, respectively. The specific heat capacity at constant pressure is denoted by c_p. Note that the subscript j represents that the parameter is located in the thermal jacket, see Fig. 1.

The reactor temperature dynamics is expressed in Eq. (6a), where the difference between the temperatures T_f and T is the heat received or transferred due to feeding the CSTR. Also, the heat transferred between the thermal jacket and the temperature inside the reactor is expressed as the difference between T and T_j. The temperature dynamics of the jacket is given by Eq. (6b) and Eq. (6c) denotes the concentration dynamics of the substrate.

Two systems are considered for the analysis of the CSTR: i) the first one is constructed using only Eq. (6a) and Eq. (6c), by assuming that all of the coolant is at a uniform temperature T_j. In other words, the increase in coolant temperature as the coolant passes through the coil is neglected; ii) the second system is constructed by considering the temperature dynamics T_j as a state, represented in the overall third-order Eq. (6). In Table 2 are listed the symbols used in the CSTR system and their numerical values.

1.2.1 Second-order CSTR system

The CSTR system modelled by Eq. (6a) and Eq. (6c) are rewritten in the nonlinear form Eq. (1), with:

$$f(x) = \begin{bmatrix} -\frac{F}{V} - r & 0 \\ -\frac{\Delta H}{\varrho c_p} r & -\frac{F}{V} - \frac{UA}{V\varrho c_p} \end{bmatrix}, \quad g(x) = \begin{bmatrix} 0 \\ \frac{UA}{V\varrho c_p} \end{bmatrix},$$
$$a = \begin{bmatrix} \frac{F}{V} C_f \\ \frac{F}{V} T_f \end{bmatrix}, \quad h(x) = \begin{bmatrix} 0 & 1 \end{bmatrix}, \quad (8)$$

where $x = [C_S, T]^\top = [x_1, x_2]^\top \in \mathbb{R}^2$ is the state vector, $u = T_j$ is the input of the system and $y = T = x_2$ is the measurable output.

1.2.2 *Third-order CSTR system*

Now, the nonlinear third-order CSTR system represented in Eq. (6) is rewritten in the form Eq. (1), as follows:

$$f(x)=\begin{bmatrix} -\frac{F}{V}-\frac{UA}{V\varrho c_p}-\frac{\Delta H}{x_1\varrho c_p}rx_3 & \frac{UA}{V\varrho c_p} & 0 \\ \frac{UA}{V_j\varrho_j c_{pj}} & \frac{-UA}{V_j\varrho_j c_{pj}} & 0 \\ 0 & 0 & -\frac{F}{V}-r \end{bmatrix},$$
$$g(x)=\begin{bmatrix} 0 \\ \frac{T_{jin}-x_2}{V_j} \\ 0 \end{bmatrix}, a=\begin{bmatrix} \frac{F}{V}T_f \\ 0 \\ \frac{F}{V}C_f \end{bmatrix}, h(x)=\begin{bmatrix} 1 & 0 & 0 \\ 0 & 1 & 0 \end{bmatrix}. \tag{9}$$

where $x=[T,T_j,C_S]^\top=[x_1,x_2,x_3]^\top\in\mathbb{R}^3$, $u=F_j$ and $y=[T,T_j]^\top=[x_1,x_2]^\top\in\mathbb{R}^2$. The control input design is synthesized while considering the reaction temperature T and the coolant temperature entering the jacket T_j as the system output, while the concentration of the product C_S is considered the unmeasurable variable. This latter choice is considered in both CSTR systems and it is justified based on the fact that a reliable and consistent concentration measurements are typically unavailable, and the sensors are expensive. Moreover, the temperatures T and T_j are considered as critical variables to be measured in the process. Both temperatures T and T_j will be controlled by manipulating the coolant flow rate F_j. In this paper, the temperature of the substrate entering the reactor T_f and the feed concentration C_f are considered as constant variables.

1.3 *qLPV representation of the CSTR*

1.3.1 *qLPV representation of the second-order CSTR system*

The scheduling variable, which is the non-constant element in Eq. (8), is $\zeta_1(t)=r=k_0e^{(-E/Rx_2)}\in[0.011,0.142]$. These values are established by considering that the product temperature is varying from 296 K to 325 K. Experimentally, the scheduling variables are defined by the designer according to the knowledge of the system and the experimental results. These values depend on the desired range that the designer establish for the CSTR system. Then, by considering Eq. (4), the weighting functions are obtained by the following equations:

$$\mu_0^1(\zeta_1)=\frac{0.142-\zeta_1(t)}{0.142-0.011},\quad \mu_1^1(\zeta_1)=1-\mu_0^1. \tag{10}$$

For $p=1$, then $m=2$ scheduling functions are computed using Eq. (5). Note that for one scheduling variable the scheduling functions are equal to the weighting functions, as follows:

$$\rho_1(\zeta_1)=\mu_0^1(\zeta_1),\quad \rho_2(\zeta_1)=\mu_1^1(\zeta_1). \tag{11}$$

Consequently, by using the scheduling functions given by (11), the nonlinear system of the second-order CSTR is exaclty represented only in the segmented expressed in Ec. (3), by the following qLPV model:

$$\begin{aligned} \dot{x}&=\sum_{i=1}^{2}\rho_i(\zeta)(A_ix+B_iu)+a, \\ y&=Cx, \end{aligned} \tag{12}$$

with

$$A_1=\begin{bmatrix} -1.011 & 0 \\ 2.326 & -3.092 \end{bmatrix}, A_2=\begin{bmatrix} -1.142 & 0 \\ 29.707 & -3.092 \end{bmatrix},$$
$$B_1=B_2=\begin{bmatrix} 0 \\ 2.092 \end{bmatrix}, a=\begin{bmatrix} \frac{F}{V}T_f \\ \frac{F}{V}C_f \end{bmatrix}, C=\begin{bmatrix} 0 & 1 \end{bmatrix}.$$

1.3.2 *qLPV representation of the third-order CSTR system*

The scheduling variables in (9) are selected as follows:

$$\begin{aligned} \zeta_1(t)&=\frac{\Delta H}{x_1\rho c_p}rx_3\in[-0.024,-0.010], \\ \zeta_2(t)&=x_2\in[296,310], \\ \zeta_3(t)&=r\in[0.014,0.038]. \end{aligned} \tag{13}$$

These values are established by considering that the cooler mean temperature T_j is varying from 296 K to 310 K, the product temperature T is varying from 300 K to 310 K, and the product concentration C_S from 0.5 mol/L to 1 mol/L. However, the designer can modify these selected segment according to the control objective and the experimental results.

For each scheduling variable, two weighting functions are computed as follows:

$$\begin{aligned} \mu_0^1(\zeta_1)&=\frac{-0.010-\zeta_1(t)}{-0.010+0.024}, & \mu_1^1(\zeta_1)&=1-\mu_0^1, \\ \mu_0^2(\zeta_2)&=\frac{310-\zeta_2(t)}{310-296}, & \mu_1^2(\zeta_2)&=1-\mu_0^2, \\ \mu_0^3(\zeta_3)&=\frac{0.038-\zeta_3(t)}{0.038-0.014}, & \mu_1^3(\zeta_3)&=1-\mu_0^3. \end{aligned} \tag{14}$$

Therefore, for $p=3$, $m=8$ scheduling functions are computed, using Eq. (5), as the product of the

weighting functions that correspond to each local model of the CSTR, as follows:

$$\begin{aligned}
\rho_1(\zeta) &= \mu_0^1\mu_0^2\mu_0^3, \quad \rho_2(\zeta) = \mu_0^1\mu_0^2\mu_1^3,\\
\rho_3(\zeta) &= \mu_0^1\mu_1^2\mu_0^3, \quad \rho_4(\zeta) = \mu_0^1\mu_1^2\mu_1^3,\\
\rho_5(\zeta) &= \mu_1^1\mu_0^2\mu_0^3, \quad \rho_6(\zeta) = \mu_1^1\mu_0^2\mu_1^3,\\
\rho_7(\zeta) &= \mu_1^1\mu_1^2\mu_0^3, \quad \rho_8(\zeta) = \mu_1^1\mu_1^2\mu_1^3.
\end{aligned} \tag{15}$$

Following the same procedure as in the previous qLPV model design, nonlinear system Eq. (9) is written in the qLPV form Eq. (2) as:

$$\begin{aligned}
\dot{x} &= \sum_{i=1}^{8} \rho_i(\zeta)(A_i x + B_i u) + a\\
y &= Cx
\end{aligned} \tag{16}$$

with

$$A_1 = A_3 = \begin{bmatrix} -3.067 & 2.092 & 0\\ 4.184 & -4.184 & 0\\ 0 & 0 & -1.014 \end{bmatrix},$$

$$A_2 = A_4 = \begin{bmatrix} -3.067 & 2.092 & 0\\ 4.184 & -4.184 & 0\\ 0 & 0 & -1.038 \end{bmatrix},$$

$$A_5 = A_7 = \begin{bmatrix} -3.081 & 2.092 & 0\\ 4.184 & -4.184 & 0\\ 0 & 0 & -1.014 \end{bmatrix},$$

$$A_6 = A_8 = \begin{bmatrix} -3.081 & 2.092 & 0\\ 4.184 & -4.184 & 0\\ 0 & 0 & -1.038 \end{bmatrix},$$

$$B_1 = B_2 = B_5 = B_6 = \begin{bmatrix} 0\\ -0.265\\ 0 \end{bmatrix},$$

$$B_3 = B_4 = B_7 = B_8 = \begin{bmatrix} 0\\ -0.537\\ 0 \end{bmatrix},$$

$$a = \begin{bmatrix} \frac{F}{V}T_f\\ 0\\ \frac{F}{V}C_f \end{bmatrix}, \quad C = \begin{bmatrix} 1 & 0 & 0\\ 0 & 1 & 0 \end{bmatrix}.$$

1.4 FTC strategy for the CSTR system

Our interest is to design and validate in simulation the fesibility of a Fault Tolerant Control (FTC) algorithm for a CSTR system using the qLPV representation of the process. In order to achieve this goal a Fault Accommodation (FA) scheme is proposed. In Fig. 2 general FA structure for both CSTR systems is depicted. Notice here that the scheme is composed of two main blocks; i) the CSTR system, and ii) the active fault tolerant control system constructed by the fault detection, estimation and accommodation subsystems.

When the CSTR is in fault-free case only the nominal controller is applied. Once the actuator fault occurs, the Fault Estimation (FE) signal generated by a qLPV Proportional-Integral Observer (PIO) is used to detect and accommodate the actuator fault. The actuator fault is detected when the FE signal has a greater value than a predefined threshold.

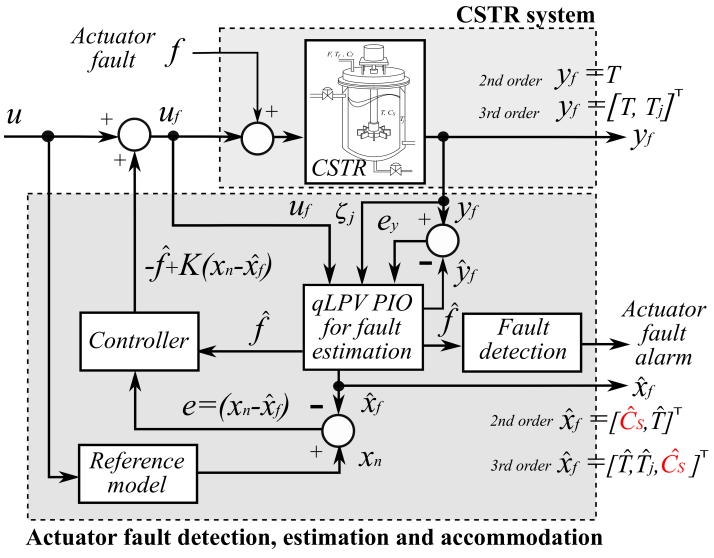

Fig. 2. Fault tolerant control scheme applied to the CSTR system.

Note that with this FTC structure the fault detection is achieved using only the fault estimation signal without generating a residual signal (Aaouaouda and Chadli, 2019). The fault accommodation control law is computed by comparing the nominal reference model and the faulty estimation system.

The error between both states is used in the controller in order to generate a new control law to reduce the effect caused by the actuator fault and to keep the stability of the CSTR system (see Fig. 2). It is important to note that the controller requires all the state vector of the CSTR to generate the control law. It means that it is necessary to estimate the product concentration C_S to compute the fault tolerant control law u_f.

1.4.1 Design of the FTC strategy for the CSTR system

The control objective of the proposed FTC system is to follow the desired trajectory generated by the nominal reference model x_n with a nominal input u, even when an actuator fault is presented in the CSTR system, accepting performance degradation in the process. The nominal reference model is expressed as:

$$\begin{aligned} \dot{x}_n &= \sum_{i=1}^{m} \rho_i(\zeta)(A_i x_n + B_i u) + a, \\ y_n &= \sum_{i=1}^{m} \rho_i(\zeta)(C_i x_n). \end{aligned} \tag{17}$$

An actuator fault can be modelled as an additive or a multiplicative external signal. For instance, multiplicative actuator fault affecting the control input can be represented by the following equation:

$$u_f = (1-\theta)u, \tag{18}$$

where θ is the actuator Loss of Effective (LoE) with $f = \theta u$, and the value of θ indicates:

$$\begin{aligned} \theta &= 1 \quad \Rightarrow \text{a total actuator fault,} \\ \theta &= 0 \quad \Rightarrow \text{the actuator is healthy,} \\ \theta &=]0,1[\quad \Rightarrow \text{LoE of the actuator.} \end{aligned}$$

In this paper, it is considered only the case of an actuator LoE presented in the CSTR system.

Now, Eq. (18) can be rewritten as an external additive fault signal as follows:

$$u_f = -f + u. \tag{19}$$

By using Eq. (19), the faulty system can be written in the following form:

$$\begin{aligned} \dot{x}_f &= \sum_{i=1}^{m} \rho_i(\zeta_f)(A_i x_f + B_i(u_f + f)) + a, \\ y_f &= \sum_{i=1}^{m} \rho_i(\zeta_f)(C_i x_f), \end{aligned} \tag{20}$$

where x_f, y_f and u_f are the faulty state vector, the faulty measured vector and the fault tolerant control input signal, respectively. The faulty scheduling function vector is represented by $\rho_i(\zeta_f)$ and it depends on the faulty scheduling variable ζ_f. The actuator fault signal is expressed by f. The presence of an actuator fault can changes abruptly the CSTR system structure and it can generate instability in the process. It means that FTC design is necessary to ensure the stability of the process.

The faulty controlled state vector x_f is affected because of the presence of the actuator fault f. As a consequence, the faulty states may differ from the nominal reference trajectory. In order to reduce this difference, the control input of the CSTR process has to be modified, and the resulting fault tolerant control input u_f is rewritten as follows:

$$u_f = -\hat{f} + K(x_n - \hat{x}_f) + u \tag{21}$$

where the controller gain is represented by K. The accommodation control law Eq. (21) is composed of three terms: i) the actuator fault estimation $\hat{f}$, ii) the difference between the nominal reference model and the faulty estimation system $x_n - \hat{x}_f$, and iii) the nominal control input u. The faulty state estimation and the actuator fault estimation is provided using a qLPV PIO, with the following structure:

$$\begin{aligned} \dot{\hat{x}}_f &= \sum_{i=1}^{m} \rho_i(\zeta_f)(A_i \hat{x}_f + B_i(u_f + \hat{f}) + H_{1i}(y_f - \hat{y}_f)) + a, \\ \dot{\hat{f}} &= \sum_{i=1}^{m} \rho_i(\zeta_f)(H_{2i}(y_f - \hat{y}_f)), \\ \hat{y}_f &= \sum_{i=1}^{m} \rho_i(\zeta_f)(C_i \hat{x}_f), \end{aligned} \tag{22}$$

where the observer gains are represented by H_{1i} and H_{2i}. Note that the qLPV observer provide the estimation of the state vector, including the product concentration C_S, that it is considered as an immeasurable variable in the process. The estimated state vector will be used to generate the control law, using the term $K(x_n - \hat{x}_f)$.

Thus, the overall scheme of the proposed FTC system, depicted in the Fig. 2, is based on the application of the control law Eq. (21) and the estimation variables using the qLPV PIO Eq. (22), such that the controller system state x_f is as close to the nominal model reference state x_n as possible. Consequently, the objective is to find the appropriate controller gain K and observer gains H_{1i} and H_{2i}, that minimize the trajectory tracking error and the state and fault estimation error, respectively, in order to ensure the stability of the CSTR process when an actuator fault is presented in the system.

Let consider the tracking error e, the state estimation error e_x and the fault estimation error e_f, respectively, defined by:

$$\begin{aligned} e &= x_n - x_f, \\ e_x &= x_f - \hat{x}_f, \\ e_f &= f - \hat{f}. \end{aligned} \tag{23}$$

Then, from Equations (17)-(22) the dynamics of the errors (22) are represented by:

$$\dot{\tilde{e}} = \begin{bmatrix} A_i - B_i K & -\tilde{L}_i \\ 0 & \tilde{A}_i - H_i \tilde{C}_i \end{bmatrix} \tilde{e} + \tilde{\Xi}\delta, \tag{24}$$

with

$$\delta = \sum_{i=1}^{m} (\rho_i(\zeta) - \rho_i(\zeta_f))(A_i x + B_i u),$$

$$\tilde{e} = \begin{bmatrix} e \\ e_x \\ e_f \end{bmatrix}, \qquad \tilde{\Xi} = \begin{bmatrix} I \\ 0 \\ 0 \end{bmatrix},$$

$$H_i = \begin{bmatrix} H_{1i} \\ H_{2i} \end{bmatrix}, \qquad \tilde{L}_i = \begin{bmatrix} B_i K & B_i \end{bmatrix},$$

$$\tilde{A}_i = \begin{bmatrix} A_i & B_i \\ 0 & 0 \end{bmatrix}, \qquad \tilde{C}_i = \begin{bmatrix} C_i & 0 \end{bmatrix}.$$

The following result gives a sufficient LMI condition to guarantee the global asymptotic convergence of $\tilde{e}$ to zero in order to compute the controller gain K and the observer gains H_{1i} and H_{2i}.

Theorem 1. (Ichalal *et al.,* 2012) The error system Eq. (24) that generates the state tracking error e and the state and fault estimation errors e_x and e_f, respectively, is stable and the $\mathcal{L}_2$-gain of the transfer from δ to e is bounded if there exists a positive scalar λ, symmetric and positive definite matrices X_1, X_2, P_2, matrices $\bar{H}, \bar{K}$ and a positive scalar $\bar{\gamma}$ solution to the following optimization problem:

$$\min_{X_1, X_2, P_2, \bar{H}, \bar{K}} \quad \bar{\gamma}, \tag{25}$$

subject to

$$\begin{aligned} \Gamma_{ii} &< 0, \\ \frac{1}{m-1}\Gamma_{ii} + \Gamma_{ij} + \Gamma_{ji} &< 0, \end{aligned} \tag{26}$$

where $i < j$, $i = 1, 2, \ldots, m$ and $j = 1, 2, \ldots, m$, with

$$\Gamma_{ij} = \begin{bmatrix} \Psi_i & -B_i M & 0 & I & X_1 \\ -M^\top B_i^\top & -2\lambda X & \lambda I & 0 & 0 \\ 0 & \lambda I & \Delta_{ij} & 0 & 0 \\ I & 0 & 0 & -\bar{\gamma} I & 0 \\ X_1^\top & 0 & 0 & 0 & -I \end{bmatrix} < 0,$$

$$\begin{aligned} \Psi_i &= \mathsf{He}\{A_i X_1 - B_i \bar{K}\}, \\ \Delta_{ij} &= \mathsf{He}\{P_2 \tilde{A}_i - \bar{H}_i \tilde{C}_{ij}\}, \\ M &= \begin{bmatrix} \bar{K} & X_2 \end{bmatrix}, \\ X &= \begin{bmatrix} X_1 & 0 \\ 0 & X_2 \end{bmatrix}, \end{aligned}$$

where $\mathsf{He}\{A_i X_1 - B_i \bar{K}\} = (A_i X_1 - B_i \bar{K}) + (A_i X_1 - B_i \bar{K})^\top$, equivalent for $\mathsf{He}\{P_2 \tilde{A}_i - \bar{H}_i \tilde{C}_{ij}\}$. I is an identity matrix with proper dimension. Then, the controller and observer gains are computed by:

$$\begin{aligned} H_i &= \begin{bmatrix} H_{1i} \\ H_{2i} \end{bmatrix} = P_2^{-1} \bar{H}_i, \\ K &= \bar{K} X_1^{-1}, \end{aligned} \tag{27}$$

and the $\mathcal{L}_2$-gain from δ to the tracking error e is obtained by

$$\bar{\gamma} = \sqrt{\gamma}. \tag{28}$$

1.4.2 Fault detection system

The actuator additive fault estimation signal f is used to detect the actuator fault at any time, as follows:

$$\begin{aligned} |\hat{f}| \geq \alpha \quad &\Rightarrow \text{in faulty case (Alarm = 1)}, \\ |\hat{f}| < \alpha \quad &\Rightarrow \text{in fault-free case (Alarm = 0)}, \end{aligned} \tag{29}$$

where α is a constant threshold, chosen according to experimental results. In fault-free case the estimated value $|\hat{f}|$ is close to zero, while in faulty case the estimated value has a greater value than the threshold, for indicating a fault occurrence. If the fault estimation value is greater than the threshold then it is considered a faulty case and the alarm indicator is one.

2 Results and discussion

In order to validate the proposed concentration estimation and the FTC strategy, four scenarios were considered: i) a CSTR nonlinear model validation is presented, ii) a comparison between the nonlinear, linear and the qLPV representation is performed, iii) a nominal scenario in order to validate the product concentration estimation is given, and finally iv) an actuator fault is injected in the process and the performance is evaluated by comparing the CSTR system without and with the FTC system. It is important to note that the FTC strategy is applied in simulation to the validated nonlinear CSTR system.

The parameters of the CSTR systems (second and third-order CSTR) used in the simulation are introduced in Table 2. Initial conditions considered for the three representations (nonlinear, linear and qLPV) are given in Table 3, and the initial conditions for each qLPV PIO are presented in Table 4.

Controller and observer gains for Eq. (21) and Eq. (22) are obtained by solving the LMI of the Theorem 1 using the Yalmip Toolbox (Lofberg *et al.,* 2004), and results in the following matrices for the second-order CSTR system:

$$K = \begin{bmatrix} 0.495 & 6.585 \end{bmatrix}, \gamma = 1.334,$$

$$H_1 = \begin{bmatrix} 0.095 \\ -0.101 \\ 0.160 \end{bmatrix}, H_2 = \begin{bmatrix} 0.683 \\ 0.016 \\ 0.632 \end{bmatrix},$$

and the gains for the third-order CSTR system are:

$$K = \begin{bmatrix} -4.608 & -3.505 & -0.001 \end{bmatrix}, \gamma = 0.960,$$

$$H_1, H_2, H_5, H_6 = \begin{bmatrix} -1.691 & 5.024 \\ 1.004 & -2.689 \\ 0.001 & -0.001 \\ 1.488 & -0.767 \end{bmatrix},$$

$$H_3, H_4, H_7, H_8 = \begin{bmatrix} -1.656 & 5.046 \\ 1.023 & -2.584 \\ 0.001 & -0.001 \\ 1.465 & -0.922 \end{bmatrix}.$$

2.1 CSTR nonlinear model validation

A comparison between CSTR process data and the nonlinear model (6) is presented in order to validate the CSTR mathematical model. The CSTR process data are obtained from Seborg *et al.,* (2010). The mathematical equations are solved in MATLAB using Euler method over a 10 min horizon and a fixed step time of 0.001 sec. The experiment consists in a step change in the coolant temperature T_j in positive and negative directions. Table 2 shows the parameters for the CSTR system.

Table 3. Nonlinear, linear and qLPV CSTR initial conditions.

Second-order CSTR			
Variable	Parameter	Value	Unit
$x_1(0)$	$C_S(0)$	0.988	mol/L
$x_2(0)$	$T(0)$	296.6	K
$u(0)$	$T_j(0)$	292	K
	T_f	350	K
	C_f	1	mol/L
Third-order CSTR			
$x_1(0)$	$T(0)$	300	K
$x_2(0)$	$T_j(0)$	298	K
$x_3(0)$	$C_S(0)$	0.7	mol/L
$u(0)$	$F_j(0)$	15	L/min
	T_f	303	K
	C_f	1	mol/L

Table 4. qLPV PIO initial conditions.

Second-order CSTR			
Variable	Parameter	Value	Unit
$\hat{x}_{f_1}(0)$	$\hat{C}_S(0)$	0.5	mol/L
$\hat{x}_{f_2}(0)$	$\hat{T}(0)$	300	K
	$\hat{f}(0)$	1	K
Third-order CSTR			
$\hat{x}_{f_1}(0)$	$\hat{T}(0)$	296.15	K
$\hat{x}_{f_2}(0)$	$\hat{T}_j(0)$	290	K
$\hat{x}_{f_3}(0)$	$\hat{C}_S(0)$	1.2	mol/L
	$\hat{f}(0)$	1	L/min

Table 5. Performance indexes between process data and nonlinear model simulation.

Quality indicator IAE		
Error	Input step change	
	$T_j = 290$ K	$T_j = 305$ K
$C_S - C_{Sp}$	0.0039	0.2026
$T - T_p$	0.2760	0.3710

[1] IAE: Integral of Absolute Error, C_{Sp}: Reactor concentration from process data, T_p: Reactor temperature from process data.

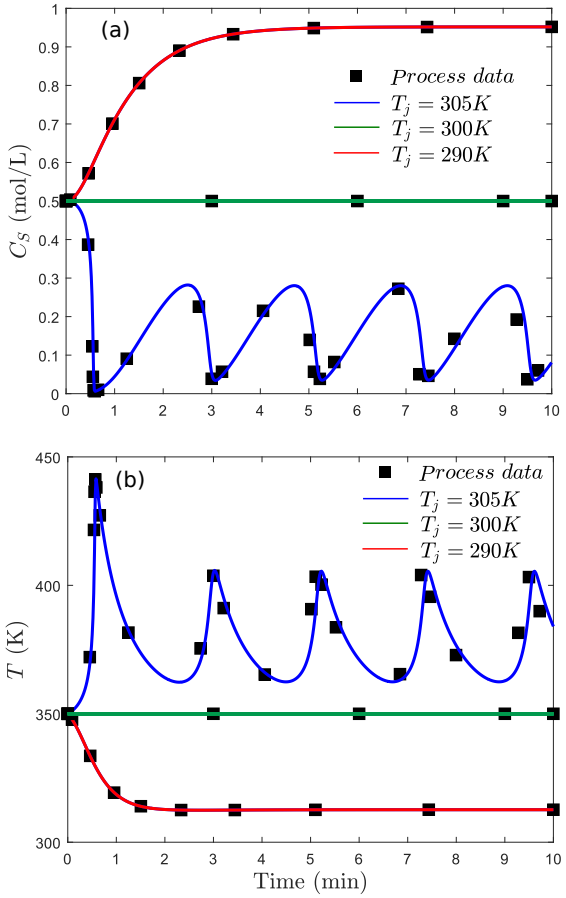

Fig. 3. Comparison between process data and nonlinear model simulation: (a) Reactor concentration, (b) Reactor temperature.

The results of the CSTR nonlinear model validation are depicted in Table 5 and Fig. 3. In Table 5 the performance of the CSTR nonlinear system is presented by using the Integral of Absolute Error (IAE) between the process data and the nonlinear model simulation. Fig. 3 shows the rector temperature and concentration as a function of time. Also, Fig. 3 depicts an oscillatory response due a jacket temperature of 305 K. By analyzing these results, it can be concluded that the mathematical model presented in this paper can be used to design an effective FTC strategy for CSTR systems.

2.2 *Comparison between nonlinear, linear and qLPV model of the CSTR system*

In this subsection a comparison between the nonlinear, linear and qLPV representation of the CSTR systems is presented in order to validate the qLPV approach to be applied in the design of the FTC system. For comparison propose we select the first linear model of the qLPV representation which is only one operation point of the CSTR process. In Fig. 4 and Fig. 5 a states comparison between the nonlinear, linear and the qLPV model for the second and third-order CSTR are displayed, respectively.

It is clear that the qLPV representation matches the nonlinear behavior correctly. Also, these figures illustrates that the linear model has bigger differences respect to the nonlinear model and the qLPV approach presents better performance to represent the nonlinear system compared to the linear one. We conclude that the qLPV system is an effective alternative for the representation of the nonlinear dynamics of the CSTR systems and it can be used for the design of the proposed FTC strategy.

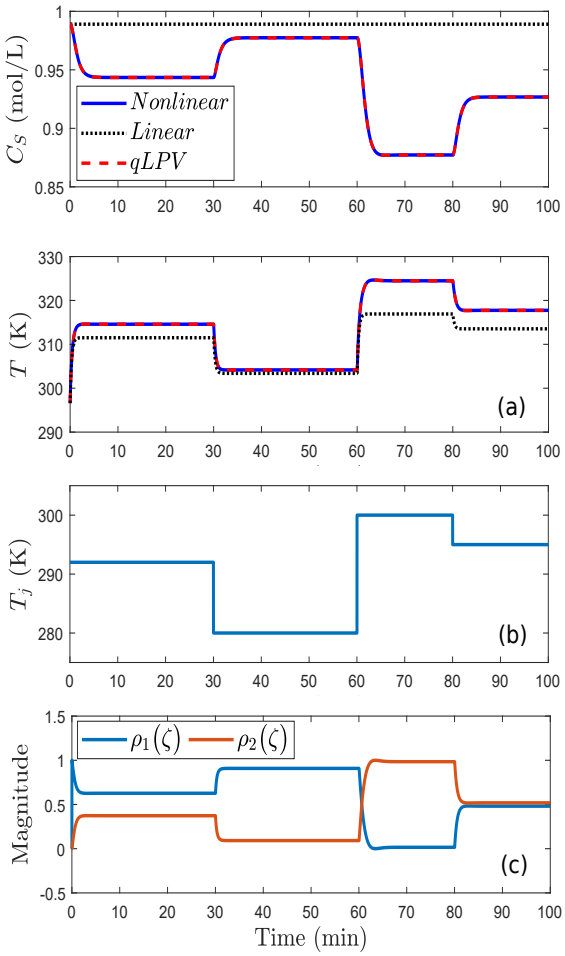

Fig. 4. (a) State comparison between nonlinear, linear and qLPV second-order CSTR, (b) Control input for nonlinear, linear and qLPV second-order CSTR, and (c) Gain scheduling functions for the qLPV model.

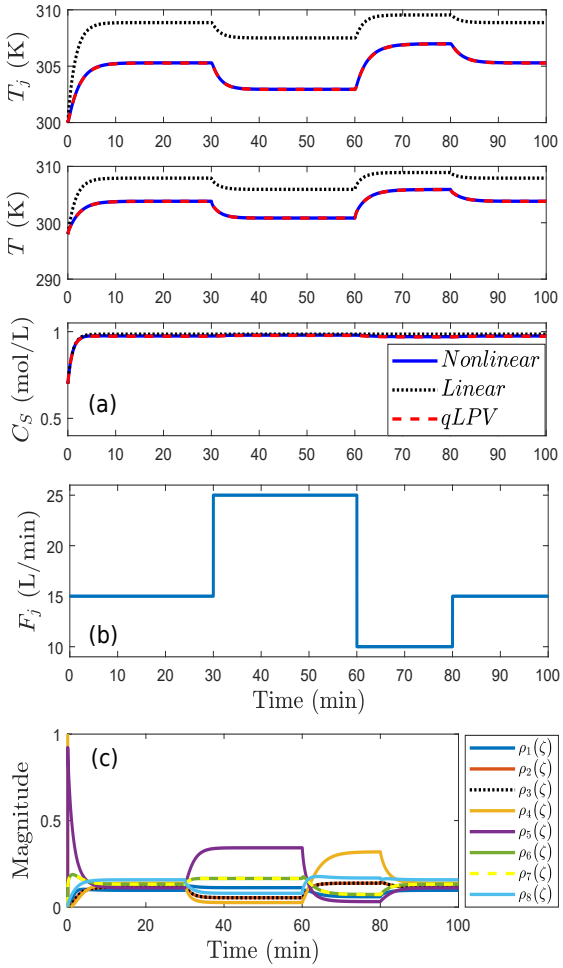

Fig. 5. (a) State comparison between nonlinear, linear and qLPV third-order CSTR, (b) Control input for nonlinear, linear and qLPV third-order CSTR, and (c) Gain scheduling functions for the qLPV model.

Additionally, in Fig. 4(b) and Fig. 5(b) the control input of each CSTR system are presented. Fig. 4(c) and Fig. 5(c) show the scheduling functions which represent the soft interpolation between the models in order to reproduce the nonlinear behavior of each CSTR system.

2.3 *Concentration estimation for the CSTR system*

In this scenario the CSTR process is considered in fault-free case and only the product concentration estimation is analyzed. The initial conditions for the qLPV observers are given in Table 4.

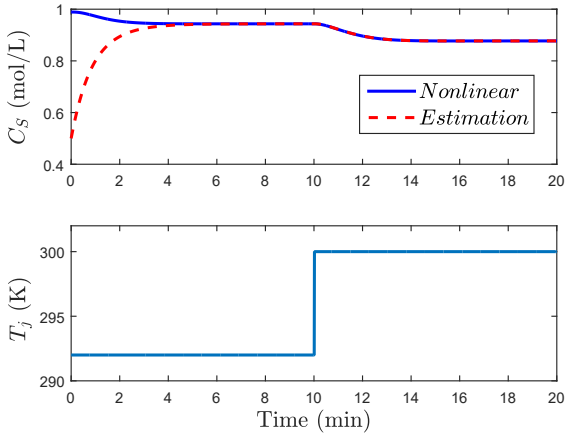

Fig. 6. Product concentration estimation and control input for the second-order CSTR system.

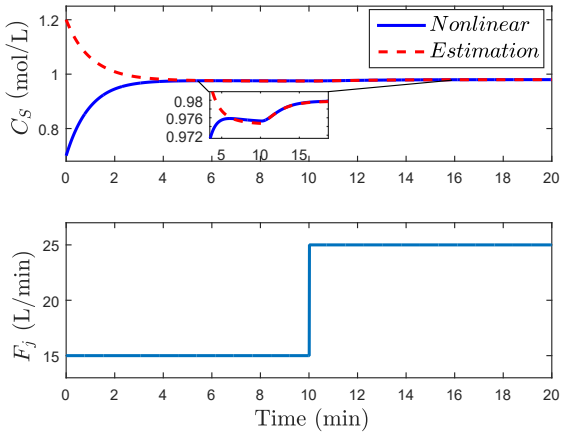

Fig. 7. Product concentration estimation and control input for the third-order CSTR system.

The concentration estimation for the second and third-order CSTR systems are presented in Fig. 6 and Fig. 7, respectively. For both systems, the observer product concentration converges fast to the real one and with small errors. Thus, the qLPV observer Eq. (22) is used, not only for state estimation but also for fault estimation. The nominal control input is depicted on the bottom part of Fig. 6 and Fig. 7.

2.4 *FTC for the CSTR system*

In this scenario an actuator fault f is injected to the second-order CSTR system as follows:

$$f = \begin{cases} 0, & t < 100, \\ 2 + \sin(t/30), & 100 \leq t \leq 300, \\ 5, & 300 < t, \end{cases} \tag{30}$$

and for the third-order CSTR system:

$$f = \begin{cases} 0, & t < 100, \\ 5 + \sin(t/30), & 100 \le t \le 300, \\ 15, & 300 < t. \end{cases} \quad (31)$$

From Fig. 8(a) and Fig. 9(a) a comparison between the model reference and the faulty CSTR system with and without the fault tolerant controller using the fault estimation generated by qLPV PIO is displayed. Notice from these figures that the error between the model reference and the states is bigger when the FTC is not applied.

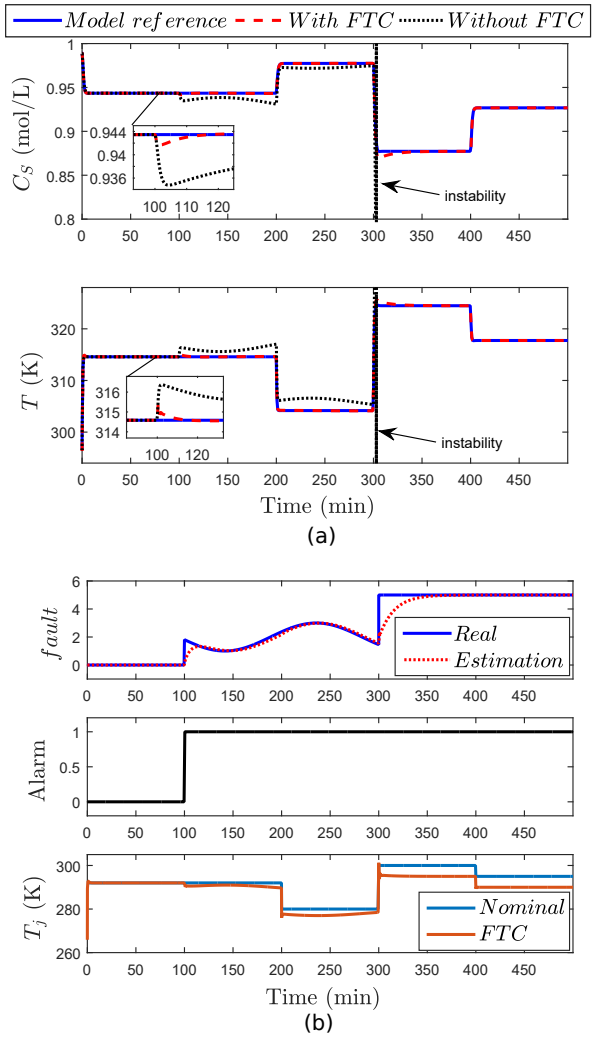

Fig. 8. (a) Comparison between the faulty second-order CSTR system with and without FTC strategy, (b) Additive fault estimation, alarm indicator and control input.

In addition, as seen in Fig. 8(a), the second-order CSTR system become unstable at 300 min, due to the presence of the actuator fault, when the proposed FTC is not applied.

In the top part of Fig. 8(b) and Fig. 9(b) the estimated additive fault and the fault detection used for generating the FA control law Eq. (21) are introduced. Observe here that shortly after the fault is injected, the magnitude estimation reasonably approximates the true fault magnitude.

Before the occurrence of an actuator fault, the additive fault estimation signal remain bellow the threshold, when the fault occurs, fault estimation value exceeds its threshold, indicating the occurrence of an actuator fault.

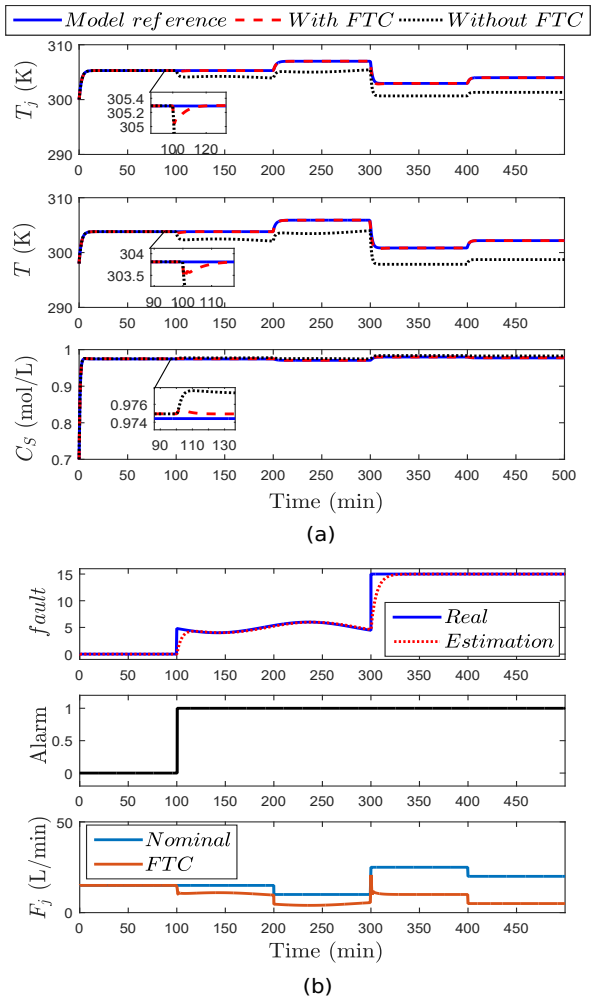

Fig. 9. (a) Comparison between the faulty third-order CSTR system with and without FTC strategy, (b) Additive fault estimation, alarm indicator and control input.

The bottom part of Fig. 8(b) and Fig. 9(b) depict the nominal control u and the FTC u_f. Even if an actuator fault occurs, the CSTR system trajectory follows the reference model, which represents the trajectory of the system in the fault-free situation. Thus, the FTC control law compensates the fault and allows normal performance of the CSTR systems in the presence of faults.

Conclusions

A product concentration estimation and an actuator fault tolerant control based on fault estimation for CSTR process were proposed in this paper. The CSTR nonlinear model is validated by comparing it with CSTR process data. Product concentration estimation strategy were simulated using a model-based observer for a second and third-order CSTR process. Then, a comparison between nonlinear, linear and qLPV CSTR system have been presented. The results demonstrate that the qLPV representation reproduce the nonlinear behavior of each CSTR systems. A qLPV PIO was used into the CSTR systems in order to simultaneously estimate the state variables and the actuator fault. Then, a fault accommodation control law was introduced using the state and fault estimation to track a reference trajectory given by a fault-free reference model. Furthermore, the qLPV PIO and the tracking error system was analyzed for ensure the stability of the scheme. Finally, simulation results have corroborated the effectiveness of the proposed FTC strategy.

References

Abdullah, A., Zribi, M. (2013). Sensor-fault-tolerant control for a class of linear parameter varying systems with practical examples. *IEEE Transactions on Industrial Electronics 60* (11), 5239–5251.

Adam-Medina, M., Escobar, R., Juárez-Romero, D., Guerrero-Ramírez, G., López-Zapata, B. (2013). Detección de fallas en un intercambiador de calor, utilizando observadores por modos deslizantes de segundo orden. *Revista Mexicana de Ingeniería Química 12* (2), 327–336.

Ahammed, A., Azeem, M. (2019). Robust stabilization and control of takagi-sugeno fuzzy systems with parameter uncertainties and disturbances via state feedback and output feedback. *International Journal of Fuzzy Systems 21* (8), 2556–2574.

Alshammari, O., Mahyuddin, M., Jerbi, H. (2020). A neural network-based adaptive backstepping control law with covariance resetting for asymptotic output tracking of a CSTR plant. *IEEE Access 8*, 29755–29766.

Alshammari, O., Mahyuddin, M., Jerbi, H. (2019). An advanced pid based control technique with adaptive parameter scheduling for a nonlinear CSTR plant. *IEEE Access 7*, 158085–158094.

Amin, E., Hasan, K. (2019). A review of fault tolerant control systems: advancements and applications. *Measurement 143*, 58–68.

Aouaouda, S., Chadli, M. (2019). Robust fault tolerant controller design for takagi-sugeno systems under input saturation. *International Journal of Systems Science 50* (6), 1163–1178.

Asadi, S., Khayatian, A., Dehghani, M., Vafamand, N., Khooban, M. (2020). Robust sliding mode observer design for simultaneous fault reconstruction in perturbed takagi-sugeno fuzzy systems using non-quadratic stability analysis. *Journal of Vibration and Control*, 1–14.

Blanke, M., Kinnaert, M., Lunze, J., Staroswiecki, M., Schroder, J. (2006). *Diagnosis and Fault-tolerant Control*. Springer. Berlin.

Boudjellal, M., Illoul, R. (2019). Design of a robust observer with super-twisting algorithm for simultaneous concentration estimation and faults reconstruction in a cstr. *International Journal of Chemical Reactor Engineering 17* (8).

Daher, A., Hoblos, G., Khalil, M., Chetouani, Y. (2020). New prognosis approach for preventive and predictive maintenance-application to a distillation column. *Chemical Engineering Research and Design 153*, 162–174.

Ebrahimi, M., Mazinan, A., Hamidi, H. (2019). Takagi-Sugeno fuzzy-based cnf control approach considering a class of constrained nonlinear systems. *IETE Journal of Research 65* (6), 872–886.

García-Morales, J., Adam-Medina, M., Escobar, R., Astorga-Zaragoza, C., García-Beltrán, C. (2015). Diagnóstico de fallas múltiples en los sensores de un intercambiador de calor empleando observadores por modos deslizantes basado en el algoritmo super-twisting. *Revista Mexicana de Ingeniería Química 14* (2), 553–565.

Gholizadeh, M., Yazdizadeh, A., Mohammad-Bagherpour, H. (2019). Fault detection and identification using combination of ekf and neuro-fuzzy network applied to a chemical process (cstr). *Pattern Analysis and Applications 22* (2), 359–373.

Hernández-Osorio, M., Ochoa-Velasco, C., García-Alvarado, M., Escobedo-Morales, A., Ruiz-López, I. (2020). Sequential synthesis of pid controllers based on lqr method. *Revista Mexicana de Ingeniería Química 19* (2), 913–928.

Ichala, D., Marx, B., Ragot, J., Maquin, D. (2012). New fault tolerant control strategies for nonlinear takagi-sugeno systems. *International Journal of Applied Mathematics and Computer Science 22* (1), 197–210.

Llanes-Santiago, O., Rivero-Benedico, B., Gálvez-Viera, S., Rodríguez-Morant, E., Torres-Cabeza, R., Silva-Neto, A. (2019). A fault diagnosis proposal with online imputation to incomplete observations in industrial plants. *Revista Mexicana de Ingeniería Química 18* (1), 83–98.

Lofberg, J. (2004). Yalmip: A toolbox for modeling and optimization in matlab. *In Computer Aided Control Systems Design, 2004 IEEE International Symposium*. 284–289.

Martínez-García, C., Puig, V., Astorga-Zaragoza, C., Madrigal-Espinosa, G., Reyes-Reyes, J. (2020). Estimation of actuator and system faults via an unknown input interval observer for takagi-sugeno systems. *Processes 8* (1), 61.

Marx, B., Ichalal, D., Ragot, J., Maquin, D., Mammar, S. (2019). Unknown input observer for LPV systems. *Automatica 100*, 67–74.

Ohtake, H., Tanaka, K., Wang, H. (2003). Fuzzy modeling via sector nonlinearity concept. *Integrated Computer-Aided Engineering 10* (4), 333–341.

Rodrigues, M., Hamdi, H., Braiek, N., Theilliol, D. (2014). Observer-based fault tolerant control design for a class of lpv descriptor systems. *Journal of the Franklin Institute 351* (6), 3104–3125.

Rotondo, D., Puig, V., Nejjari, F., Witczak, M. (2015). Automated generation and comparison of takagi-sugeno and polytopic quasi-lpv models. *Fuzzy Sets and Systems 277*, 44–64.

Rumbo-Morales, J., Lopez-Lopez, G., Alvarado, V., Valdez-Martinez, J., Sorcia-Vázquez, F., Brizuela-Mendoza, J. (2018). Simulation and control of a pressure swing adsorption process to dehydrate ethanol. *Revista Mexicana de Ingeniería Química 17*, 1051-1081.

Rumbo-Morales, J., Perez-Vidal, A., Ortiz-Torres, G., Salas-Villalobo, A., Sorcia-Vázquez, F., Brizuela-Mendoza, J., De-la-Torre, M., Valdez-Martínez, J. (2020). Adsorption and separation of the H_2O/H_2SO_4 and H_2O/C_2H_5OH mixtures: a simulated and experimental study. *Processes 8* (3), 290.

Seborg, D., Mellichamp, D., Edgar, T., Doyle, F. (2010). *Process Dynamics and Control*. John Wiley and Sons.

Simkoff, J., Baldea, M. (2019). Production scheduling and linear mpc: complete integration via complementarity conditions. *Computers and Chemical Engineering 125*, 287–305.

Sorcia-Vázquez, F., García-Beltrán, C., Valencia-Palomo, G., Brizuela-Mendoza, J., Rumbo-Morales, J. (2020). Decentralized robust tube-based model predictive control: application to a four-tank-system. *Revista Mexicana de Ingeniería Química 19* (3), 1135–1151.

Tamboli, D., Chile, R. (2018). Multi-model approach for 2-dof control of nonlinear cstr process. *International Journal of Modelling, Identification and Control 30* (2), 143–161.

Tanaka, K., Ohtake, H., Wang, H. (2006). Recursive pointwise design for nonlinear systems. *IEEE Transactions on Fuzzy Systems 14* (2), 305–3013.

Wan, Y., Puig, V., Ocampo-Martinez, C., Wang, Y., Harinath, E., Braatz, R. (2020). Fault detection

for uncertain lpv systems using probabilistic set-membership parity relation. *Journal of Process Control 87*, 27–36.

Wang, Y., Pan, Z., Yuan, X., Yang, C., Gui, W. (2020). A novel deep learning based fault diagnosis approach for chemical process with extended deep belief network. *ISA transactions 96*, 457–467.

Yazdi, S., Khayatian, A. (2020). Performance improvement by optimal reset dynamic output feedback control based on model predictive strategy. *Journal of Process Control 88*, 78–85.

Zerari, N., Chemachema, M. (2019). Robust adaptive neural network prescribed performance control for uncertain cstr system with input nonlinearities and external disturbance. *Neural Computing and Applications*, 1–14.

Zhang, Y., Jiang, J. (2008). Bibliographical review on reconfigurable fault-tolerant control systems. *Annual Reviews in Control 32* (2), 229–252.

Zhang, J., Christofides, P., He, X., Albalawi, F., Zhao, Y., Zhou, D. (2020). Intermittent sensor fault detection for stochastic ltv systems with parameter uncertainty and limited resolution. *International Journal of Control 93* (4), 788–796.

Zheng, W., Wang, H., Zhang, Z., Wen, S., Wang, Y. (2020). Dynamic output-feedback control for chemical stirred tank reactor system with multiple time-delays: a Lyapunov-Krasovskii functional approach. *International Journal of Computational Methods 17* (2), 1850138.